# Development data associated with effects of stiffness softening of 3D-TIPS elastomer nanohybrid scaffolds on tissue ingrowth, vascularization and inflammation in vivo

Linxiao Wu, Adrián Magaz, Elizabeth Maughan, Nina Oliver, Arnold Darbyshire, Marilena Loizidou, Mark Emberton, Martin Birchall, Wenhui Song

www.elsevier.com/locate/dib

PII: S2352-3409(19)30013-7S1742-7061(18)30744-X
DOI: https://doi.org/10.1016/j.dib.2019.01.012
Reference: DIB3664

To appear in: *Data in Brief*

Received date: 15 December 2018
Revised date: 28 December 2018
Accepted date: 4 January 2019

Cite this article as: Linxiao Wu, Adrián Magaz, Elizabeth Maughan, Nina Oliver, Arnold Darbyshire, Marilena Loizidou, Mark Emberton, Martin Birchall and Wenhui Song, Development data associated with effects of stiffness softening of 3D-TIPS elastomer nanohybrid scaffolds on tissue ingrowth, vascularization and inflammation in vivo, *Data in Brief,* https://doi.org/10.1016/j.dib.2019.01.012

*Data article*

**Title:** Development data associated with effects of stiffness softening of 3D-TIPS elastomer nanohybrid scaffolds on tissue ingrowth, vascularization and inflammation *in vivo.*

**Authors:** Linxiao Wu[1], Adrián Magaz[1†], Elizabeth Maughan[2], Nina Oliver[1], Arnold Darbyshire[1], Marilena Loizidou[1], Mark Emberton[1], Martin Birchall[2], Wenhui Song[1*]

**Affiliations:**

[1]Centre for Biomaterials in Surgical Reconstruction and Regeneration, Division of Surgery & Interventional Science, University College London, London, NW3 2PF, United Kingdom

[2]UCL Ear Institute, Royal National Throat Nose and Ear Hospital and University College London, London, United Kingdom.

[†]Current address: Bio-Active Materials Group, School of Materials, The University of Manchester, Manchester, United Kingdom.

**Contact email:** w.song@ucl.ac.uk

**Abstract**

This DiB article contains data related to the research article entitled "Cellular responses to thermoresponsive stiffness memory elastomer nanohybrid scaffolds by 3D-TIPS" [1]. Thermoresponsive poly (urea-urethane) nanohybrid elastomer (PUU-POSS) scaffolds were implanted in rats for up to 3 months. The porous structure and tensile mechanical properties of the scaffolds are listed and compared before and after *in vitro* and *in vivo* tests. The details of histological analysis of the explants with different initial stiffness and porous structures at various time points are presented. The images and data presented support the conclusion about the coupled effects of stiffness softening and the hierarchical porous structure modulating tissue ingrowth, vascularization and macrophage polarization the article [1].



**Specifications Table**

| | |
|---|---|
| Subject area | *Chemistry, Biology* |
| More specific subject area | *Biomaterials* |
| Type of data | *Tables, Figures* |
| How data was acquired | *Static tensile mechanical testing (Instron5655), Mercury intrusion porosimeter (Quantachrome Poremaster 60GT), XRD (Bruker D8 Advance), immunohistochemistry* |
| Data format | *Analyzed* |
| Experimental factors | *Scaffolds prior to implantation were subjected to uniaxial mechanical testing and mercury intrusion porosimeter. Scaffold explants at different time points were subjected to uniaxial mechanical testing* |

| | |
|---|---|
| | *and XRD characterization. In addition, explants were sectioned and stained for Hematoxylin and Eosin (H&E) and Masson's trichrome (M&T). Immunofluorescent staining was carried out to detect presence of capillary markers (i.e. CD31), macrophage markers (i.e. CD86, CD68, CD163) and T-cell makers (i.e. CD3, CD4).* |
| Experimental features | *Physico-mechanical characterization, histology and immunohistochemistry* |
| Data source location | *Centre for Biomaterials in Surgical Reconstruction and Regeneration, Division of Surgery & Interventional Science, University College London, Royal Free Hospital London NHS Foundation Trust, London, United Kingdom, NW3 2PF* |
| Data accessibility | *Within this article* |
| Related research article | *[1] L. Wu, A. Magaz, E. Maughan, N. Oliver, A. Darbyshire, M. Loizidou, M. Emberton, M. Birchall, W. Song, Cellular responses to thermoresponsive stiffness memory elastomer nanohybrid scaffolds by 3D-TIPS, Acta Biomater. (2018). doi:10.1016/j.actbio.2018.12.019.* |

**Value of the data**

- Data presented in this article provides direct comparison of the stiffness softening and hierarchical structure of the 3D-TIPS scaffolds before and after *in vitro* and *in vivo* tests. The data magnify more insights about the changes of structures at multi-scales and mechanical properties of the scaffolds under biophysical and biological conditions.
- The histological images of the scaffolds with different initial stiffness and porous structure by immunohistochemistry elucidate for the first time how stiffness softening and digitally printed hierarchical porous structure regulate the tissue ingrowth, vascularization and macrophage polarization towards an M2 phenotype at the early (week 4) and late (week 12) stages *in vivo*.



## 1. Data

**Table 1** shows the stiffness softening effect of the scaffolds *in vitro* over day 0-28 and how they relax towards their intrinsic elasticity. The dimensions of the 3D printed preforms and the scaffolds as produced are shown in **Table 2. Tables 3-6** and **Table 7** show the effects of softening during *in vivo* implantation at various time points, in terms of tensile mechanical properties and XRD characterization respectively. **Figures 1-3** depict low and high magnification of Hematoxylin and Eosin (H&E) and Masson's trichrome (M&T) staining showing collagen fibre orientation and tissue ingrowth within the explants. **Table 8** quantifies the angiogenic response of the explants during implantation time with stiffness softening. The softening effects on macrophage polarization (M1 markers CD86, CD63 and M2 maker CD163) and T-cell response (markers CD3 and CD4) are quantified in **Tables 9-15**; representative immunohistochemistry images are shown in **Figures 4-13**.

### 1.1 Static tensile mechanical properties and hierarchical porous structure of the scaffolds

**Table 1** Stiffness softening of PUU-POSS scaffolds with 50% infill density, tested at wet condition before and after *in vitro* incubation at 37℃ over 28 days.

| 3D-TIPS scaffold, 50% infill | | Tensile Modulus (at 50% strain) MPa | Tensile Modulus (at 100% strain) MPa | Ultimate tensile strength (breaking point), MPa | Strain at break, % | Toughness, J. $m^{-3}\times10^{4}$ |
|---|---|---|---|---|---|---|
| **50CC** | Day 0 | 0.98 (±0.14) | 0.82 (±0.21) | 1.33 (±0.09) | 179 (±8) | 137 (±22) |
| | Day 28 | 0.45 (±0.08) | 0.40 (±0.11) | 0.77 (±0.15) | 230 (±13) | 115 (±20) |
| **50CC+H** | Day 0 | 0.53 (±0.02) | 0.44 (±0.08) | 0.76 (±0.05) | 236 (±19) | 113 (±27) |
| | Day 28 | 0.39 (±0.09) | 0.32 (±0.08) | 0.72 (±0.12) | 240 (±18) | 110 (±14) |
| **50RTC+H** | Day 0 | 0.44 (±0.06) | 0.39 (±0.09) | 0.67 (±0.03) | 146 (±15) | 146 (±12) |
| | Day 28 | 0.42 (±0.08) | 0.38 (±0.10) | 0.65 (±0.06) | 149 (±19) | 146(±20) |

**Table 2** Dimensions of 3D-printed PVA preforms and PUU-POSS scaffolds made by 3D-TIPS

| Scaffold | | x- Strut thickness (μm, n=10) | y-Strut thickness (μm, n=10) | z-Strut thickness (μm, n=10) | Sample Size, (L×W×T, mm) (n=6) | Apparent Volume ($mm^3$) | Volume Swelling Ratio vs $V_{PVA}$ (%) |
|---|---|---|---|---|---|---|---|
| 50% infill PVA preform (mould) | | 400 | 400 | 200 | 60.0×12.0×4.0 | 2880 ± 4 | |
| **50CC** | Wet, as produced, RT | 197±13 | 157±9 | 118±19 | 61.0×13.0×3.6 | 2855 ± 9 | -0.9 ± 0.2 |
| **50CC+H** | Wet, as produced, RT | 176±8 | 150±8 | 121±14 | 59.7×11.3×3.5 | 2361 ± 7 | -18.0 ± 0.1 |
| **50RTC+H** | Wet, as produced, RT | 186±10 | 140±11 | 127±10 | 58.9×12.7×3.9 | 2917 ± 13 | 1.2 ± 0.3 |

**Table 3** Tensile modulus (at 50% strain) of the scaffold explants at weeks 4, 8 and 12.

| **Tensile modulus (MPa)** | **50CC** | **50CC+H** | **50RTC+H** |
|---|---|---|---|
| Week 0 | 1.11 (±0.13) | 0.77 (±0.09) | 0.43 (±0.08) |
| Week 4 | 2.45 (±0.40) | 2.13 (±1.38) | 1.56 (±0.20) |
| Week 8 | 3.99 (±0.55) | 3.73 (±0.78) | 3.13 (±0.88) |
| Week 12 | 6.97 (±1.46) | 6.08 (±1.35) | 5.88 (±1.53) |

**Table 4** Strain at break of the scaffold explants at weeks 4, 8 and 12.

| **Strain at break (%)** | **50CC** | **50CC+H** | **50RTC+H** |
|---|---|---|---|
| Week 0 | 179 (±18) | 186 (±19) | 146 (±15) |
| Week 4 | 340 (±24) | 310 (±61) | 291 (±70) |
| Week 8 | 444 (±73) | 423 (±71) | 406 (±122) |
| Week 12 | 521 (±70) | 494 (±65) | 454 (±80) |

**Table 5** Ultimate tensile strength (breaking point) of the scaffold explants at weeks 4, 8 and 12.

| **Ultimate tensile strength (MPa)** | **50CC** | **50CC+H** | **50RTC+H** |
|---|---|---|---|
| Week 0 | 1.63 (±0.09) | 0.99 (±0.05) | 0.67 (±0.07) |
| Week 4 | 1.07 (±0.39) | 1.01 (±0.45) | 0.81 (±0.18) |
| Week 8 | 1.98 (±0.37) | 1.86 (±0.53) | 1.16 (±0.39) |
| Week 12 | 2.84 (±0.53) | 2.60 (±0.75) | 2.44 (±0.29) |

**Table 6** Toughness of the scaffold explants at weeks 4, 8 and 12.

| **Toughness ($J.m^{-3}$ $10^4$)** | **50CC** | **50CC+H** | **50RTC+H** |
|---|---|---|---|
| Week 0 | 137 (±12) | 146 (±12) | 113 (±17) |
| Week 4 | 412 (±24) | 370 (±66) | 351 (±79) |
| Week 8 | 523 (±73) | 463 (±81) | 406 (±162) |
| Week 12 | 599 (±99) | 524 (±77) | 444 (±90) |

**Table 7** Analysis of WAXD spectra of the explants during implantation. Degree of crystallinity (Dc, %), d-spacing (d, A) of semicrystalline structure and broad halo peaks of amorphous structures.

| **Scaffolds** | | **Week 0** | | | **Week 4** | | | **Week e8** | | | **Week 12** | | |
|---|---|---|---|---|---|---|---|---|---|---|---|---|---|
| | | **2θ** | **d** | **Dc** | **2θ** | **d** | **Dc** | **2θ** | **d** | **Dc** | **2θ** | **d** | **Dc** |
| **50CC** | **Sharp peak 1** | 20.0 | 4.4 | 37.6 | | | | | | | | | |
| | **Sharp peak 2** | 23.2 | 3.8 | | | | | | | | | | |
| | **Broad halo peak 1** | | | | | | | | | | | | |
| | **Broad halo peak 2** | | | | | | | | | | 20.1 | | |
| | **Broad halo peak 3** | | | | 30.0 | | | 30.5 | | | 31.2 | | |
| | **Broad halo peak 4** | | | | 40.5 | | | 41.5 | | | 41.9 | | |
| **50CC+H** | **Sharp peak 1** | | | | | | | | | | | | |
| | **Sharp peak 2** | | | | | | | | | | | | |
| | **Broad halo peak 1** | | | | | | | | | | | | |
| | **Broad halo peak 2** | | | | 19.2 | | | 19.2 | | | 20.0 | | |
| | **Broad halo peak 3** | 30.3 | | | 28.8 | | | 29.8 | | | 30.9 | | |
| | **Broad halo peak 4** | 41.3 | | | 42.1 | | | 42.2 | | | 42.2 | | |
| **50RTC+H** | **Sharp peak 1** | | | | | | | | | | | | |
| | **Sharp peak 2** | | | | | | | | | | | | |
| | **Broad halo peak 1** | | | | | | | | | | | | |
| | **Broad halo peak 2** | | | | | | | | | | 19.3 | | |
| | **Broad halo peak 3** | 26.0 | | | 25.9 | | | 27.0 | | | 27.1 | | |
| | **Broad halo peak 4** | 42.3 | | | 42.0 | | | 42.7 | | | 41.6 | | |

### 1.2 Cellular infiltration and matrix deposition

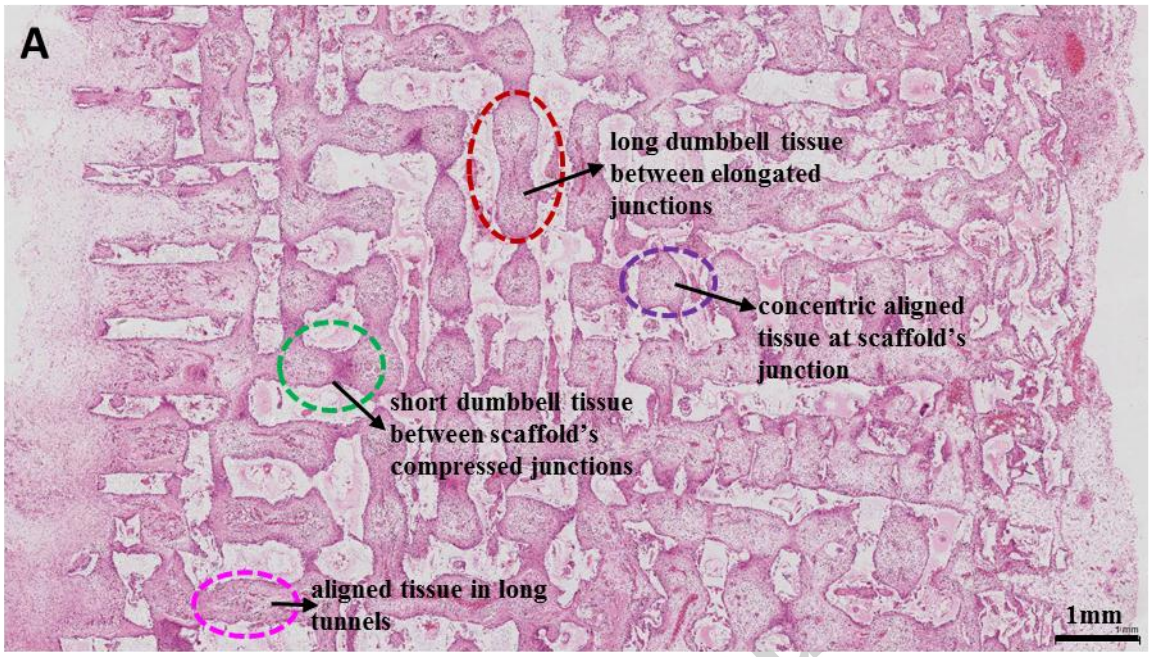


**Figure 1** Hematoxylin & Eosin (H&E) stained histological structure of middle in-plane of 50CC scaffold explants at week 12 depicting tissue ingrowth within the scaffold network, ×2 magnifications.

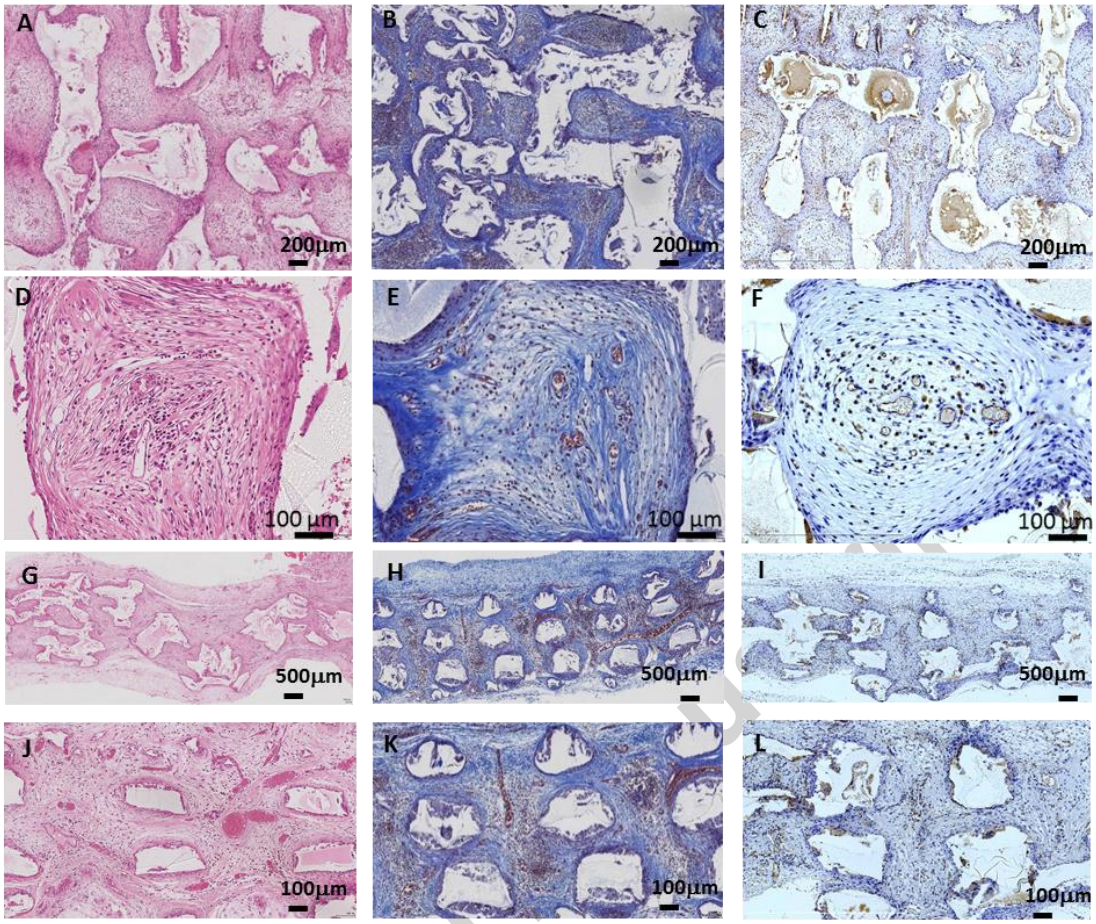


**Figure 2 Subcutaneous implantation of 50CC+H scaffolds at week 12**: (A) tissue integration of middle-in-plane of the 50CC+H scaffold by Hematoxylin and Eosin (H&E) staining, (B) collagen production by Masson's trichrome staining (M&T), (C) endothelial cell infiltration as identified by CD31 staining, used as a marker of angiogenesis; (D-F) enlarged views of middle-in-plane respectively. (G-I) Middle cross-section view and (J-L) enlarged view.

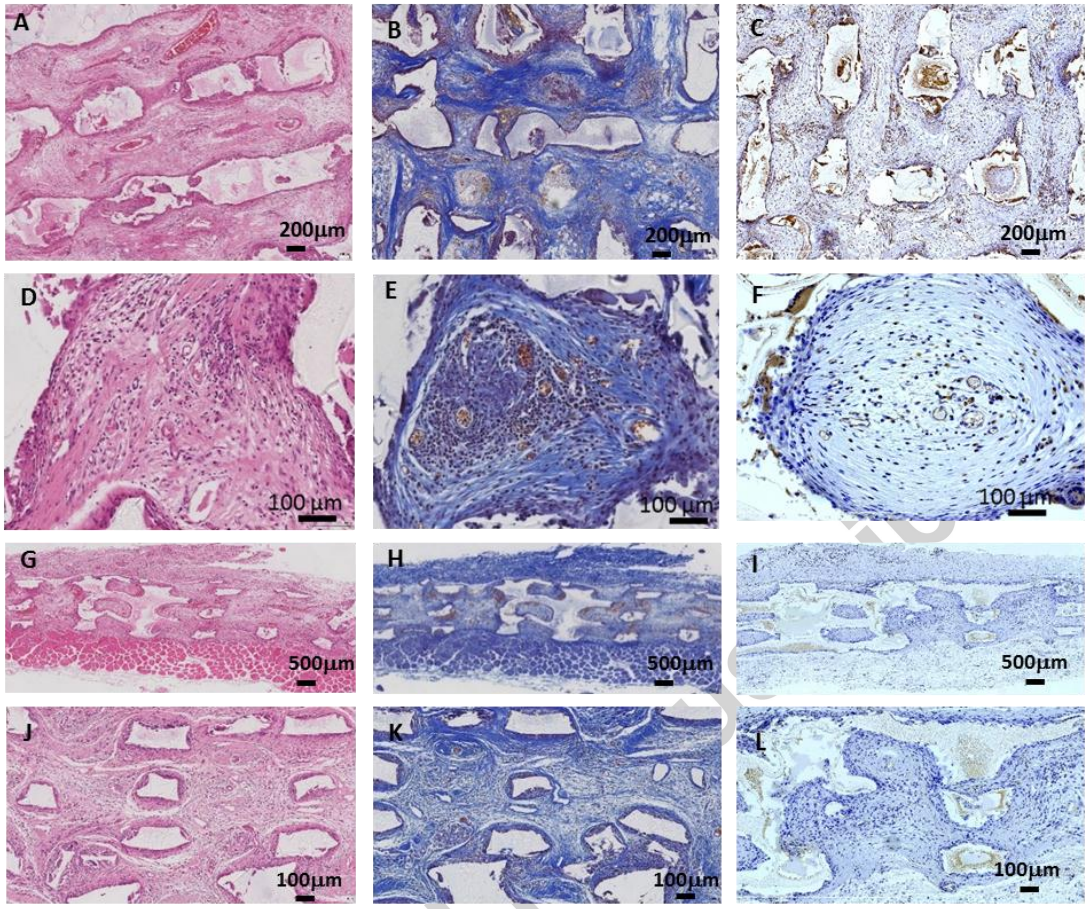


**Figure 3 Subcutaneous implantation of 50RTC+H scaffolds at week 12**: (A) tissue integration of middle-in-plane of the 50RTC+H scaffold by Hematoxylin and Eosin (H&E) staining, (B) collagen production by Masson's trichrome staining, (C) endothelial cell infiltration as identified by CD31 staining, used as a marker of angiogenesis; (D-F) enlarged views of middle-in-plane respectively. (G-I) Middle cross-section view and (J-L) enlarged view.

### 1.3 Angiogenesis response

**Table 8** Proportion of total tissue/scaffold volume occupied by blood capillaries at weeks 4, 8 and 12. Immunofluorescent staining of anti-CD31 marker for blood capillaries.

| **Capillary (%)** | **50CC** | **50CC+H** | **50RTC+H** |
|---|---|---|---|
| Week 4 | 11 (±1) | 6 (±2) | 3 (±2) |
| Week 8 | 25 (±3) | 12 (±4) | 8 (±4) |
| Week 12 | 30 (±4) | 20 (±5) | 14 (±5) |

### 1.4 T-cell proliferative and host macrophage response

**Table 9** Host pan-macrophage/monocyte response (CD68+ marker) towards the implanted scaffolds in terms of numerical density (Nv), representing the number of cells across the scaffold per unit square (Nv/mm$^2$) at week 4, 8 and 12 (n=20 frames, 12 scaffolds in each group at each time point).

| **CD68+** | **50CC** | **50CC+H** | **50RTC+H** |
|---|---|---|---|
| Week 4 | 353 (±54) | 301 (±56) | 210 (±46) |
| Week 8 | 322 (±48) | 260 (±39) | 164 (±48) |
| Week 12 | 228 (±39) | 201 (±43) | 115 (±52) |

**Table 10** Host macrophage response (CD86+ marker) towards the implanted scaffolds in terms of numerical density (Nv), representing the number of cells across the scaffold per unit square (Nv/mm$^2$) at week 4, 8 and 12 (n=20 frames, 12 scaffolds in each group at each time point).

| **CD86+** | **50CC** | **50CC+H** | **50RTC+H** |
|---|---|---|---|
| Week 4 | 397 (±56) | 289 (±47) | 152 (±39) |
| Week 8 | 312 (±55) | 224 (±51) | 132 (±45) |
| Week 12 | 271 (±41) | 186 (±55) | 96 (±53) |

**Table 11** Host macrophage response (CD163+ marker) towards the implanted scaffolds in terms of numerical density (Nv), representing the number of cells across the scaffold per unit square (Nv/mm$^2$) at week 4, 8 and 12 (n=20 frames, 12 scaffolds in each group at each time point).

| **CD163+** | **50CC** | **50CC+H** | **50RTC+H** |
|---|---|---|---|
| Week 4 | 360 (±64) | 294 (±65) | 78 (±36) |
| Week 8 | 531 (±88) | 434 (±76) | 103 (±67) |
| Week 12 | 679 (±94) | 534 (±78) | 167 (±46) |

**Table 12** Ratio of CD68+/ CD163+ of the various scaffold groups at weeks 4, 8 and 12.

| **CD68+/CD163+** | **50CC** | **50CC+H** | **50RTC+H** |
|---|---|---|---|
| Week 4 | 0.98 | 1.02 | 2.69 |
| Week 8 | 0.60 | 0.59 | 1.59 |
| Week 12 | 0.33 | 0.38 | 0.68 |

**Table 13** Ratio of CD86+/ CD163+ of the various scaffold groups at weeks 4, 8 and 12.

| **CD86+/CD163+** | **50CC** | **50CC+H** | **50RTC+H** |
|---|---|---|---|
| Week 4 | 1.10 | 0.98 | 1.95 |
| Week 8 | 0.59 | 0.52 | 1.28 |
| Week 12 | 0.40 | 0.35 | 0.57 |

**Table 14** Host T lymphocyte response (CD3+ marker) towards the implanted scaffolds in terms of numerical density (Nv), representing the number of cells across the scaffolds per unit square ($Nv/mm^2$) at week 4, 8 and 12 (n=20 frames, 12 scaffolds in each group at each time point).

| **CD3+** | **50CC** | **50CC+H** | **50RTC+H** |
|---|---|---|---|
| Week 4 | 372 (±54) | 301 (±56) | 134 (±31) |
| Week 8 | 232 (±48) | 204 (±39) | 67 (±15) |
| Week 12 | 156 (±44) | 109 (±43) | 35 (±8) |

**Table 15** Host T lymphocyte response (CD4+ marker) towards the implanted scaffolds in terms of numerical density (Nv), representing the number of cells across the scaffolds per unit square ($Nv/mm^2$) at week 4, 8 and 12 (n=20 frames, 12 scaffolds in each group at each time point).

| **CD4+** | **50CC** | **50CC+H** | **50RTC+H** |
|---|---|---|---|
| Week 4 | 301 (±61) | 245 (±71) | 152 (±27) |
| Week 8 | 252 (±42) | 201 (±46) | 102 (±28) |
| Week 12 | 122 (±32) | 87 (±45) | 32 (±16) |

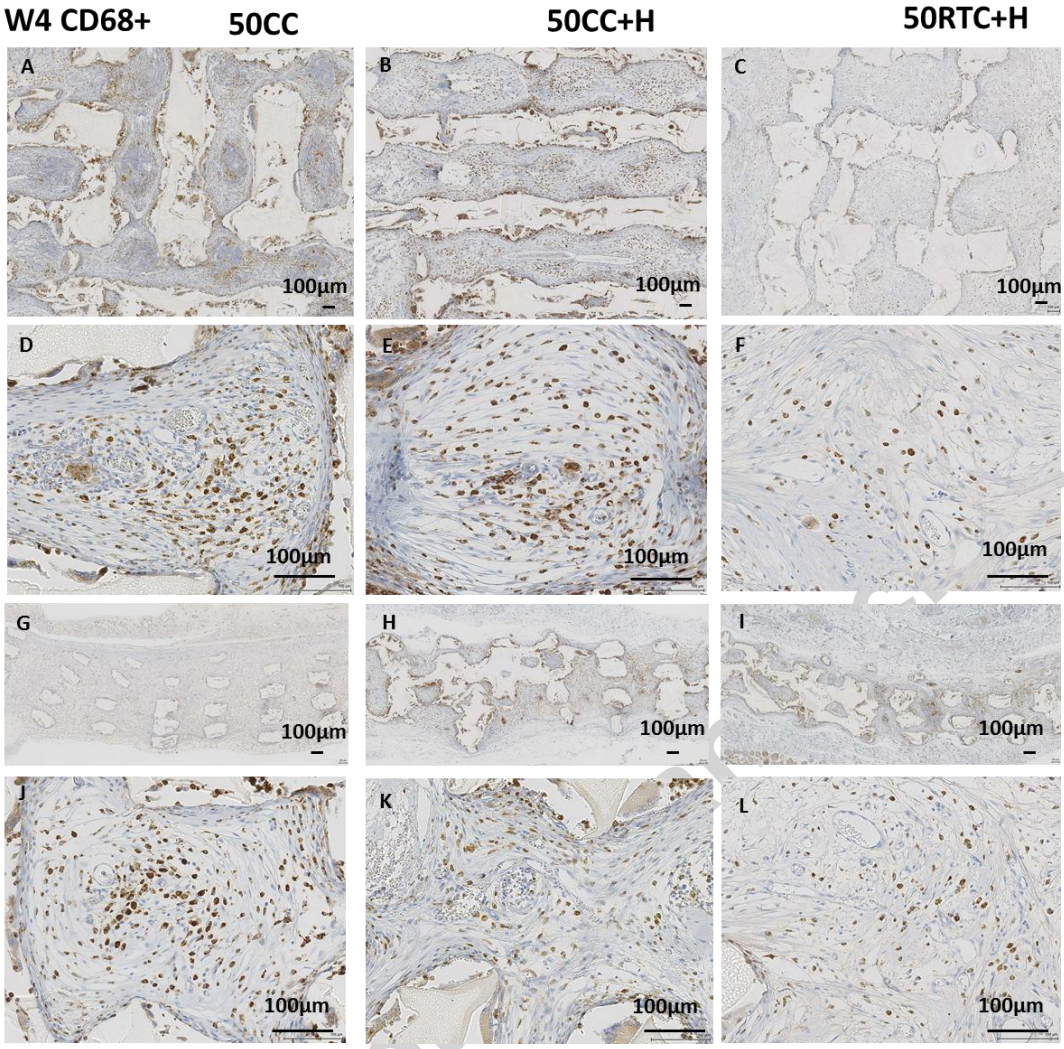


**Figure 4 Immunohistochemistry of the host macrophage response towards scaffolds *in vivo* at week 4**. Tissue integration of middle-in-plane (A-F) and cross-sectional view (G-L) of the scaffolds by CD68 (M1 pan-macrophage/monocyte marker) staining at (A-C, G-I) ×4 and (D-F, J-L) ×20 magnifications.

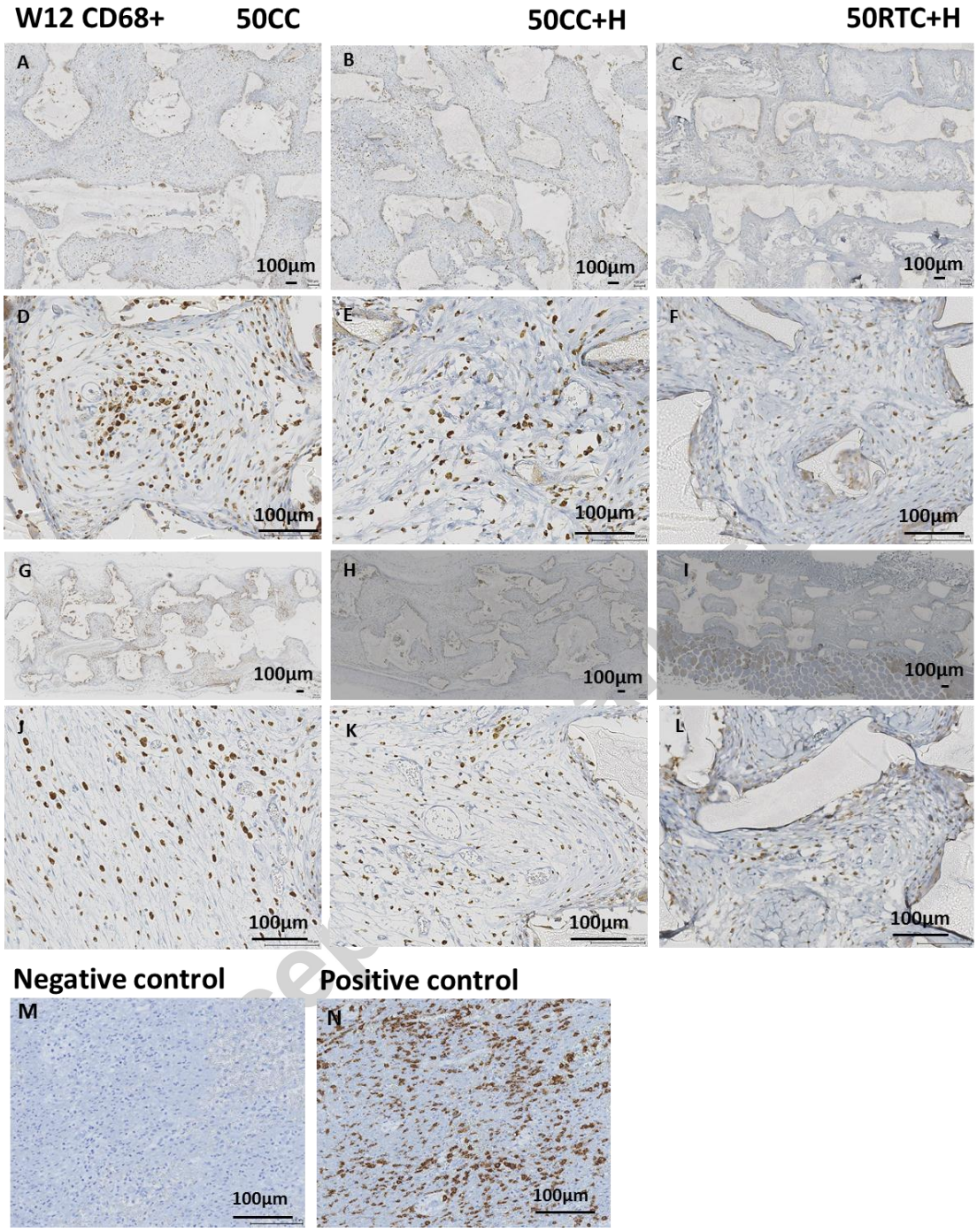


**Figure 5 Immunohistochemistry of the host macrophage response towards scaffolds *in vivo* at week 12**. Tissue integration of middle-in-plane (A-F) and cross-sectional view (G-L) of the scaffolds by CD68 (pan-macrophage/monocyte marker) staining at (A-C, G-I) ×4 and (D-F, J-I) ×20 magnifications. (M) Negative control (rat appendix); (N) positive control (rat liver). Scale bar: 100 µm.

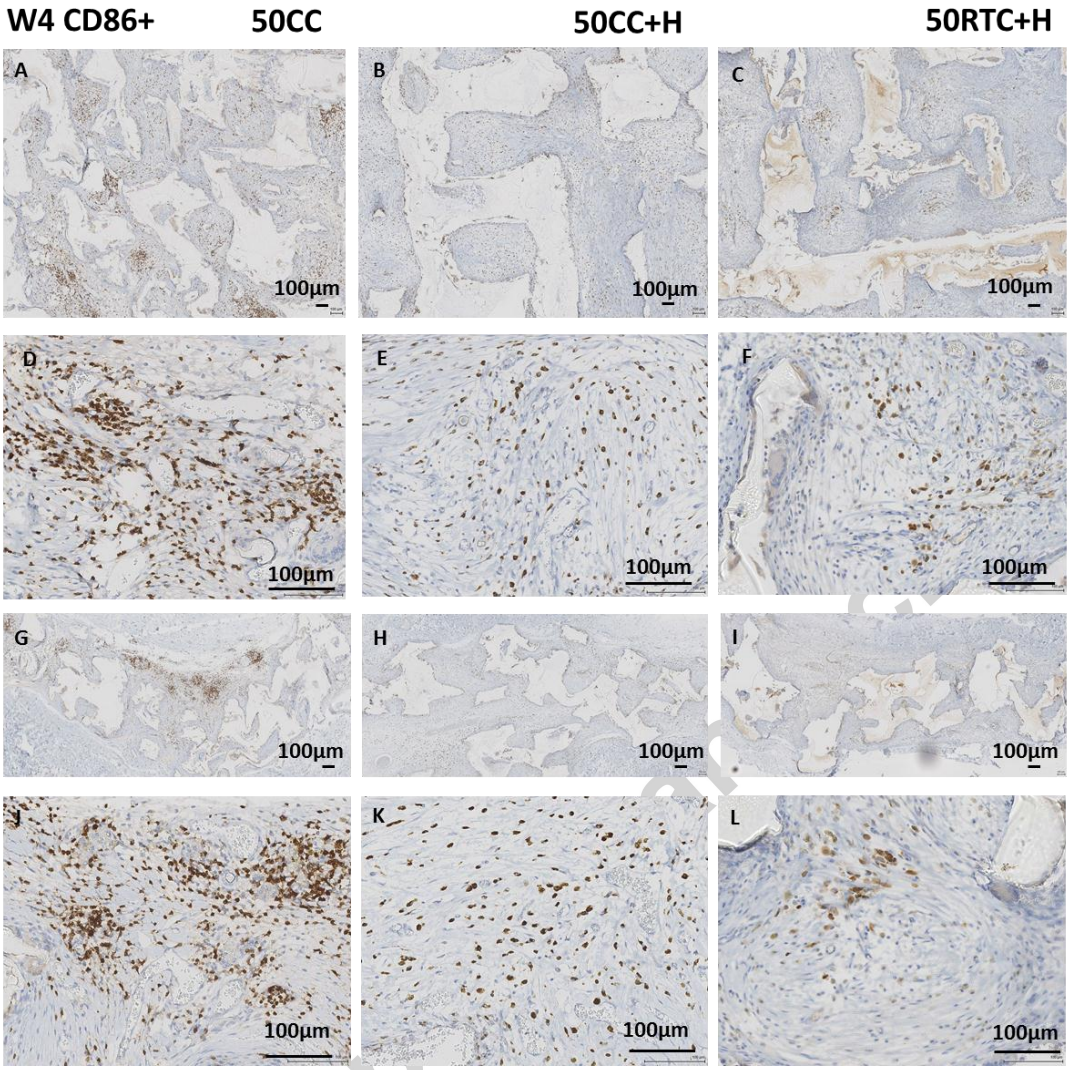


**Figure 6 Immunohistochemistry of the host macrophage response towards scaffolds *in vivo* at week 4**. Tissue integration of middle-in-plane (A-F) and cross-sectional view (G-L) of the scaffolds by CD86 (M1 macrophage marker) staining at (A-C, G-I) ×4 and (D-F, J-L) ×20 magnifications.

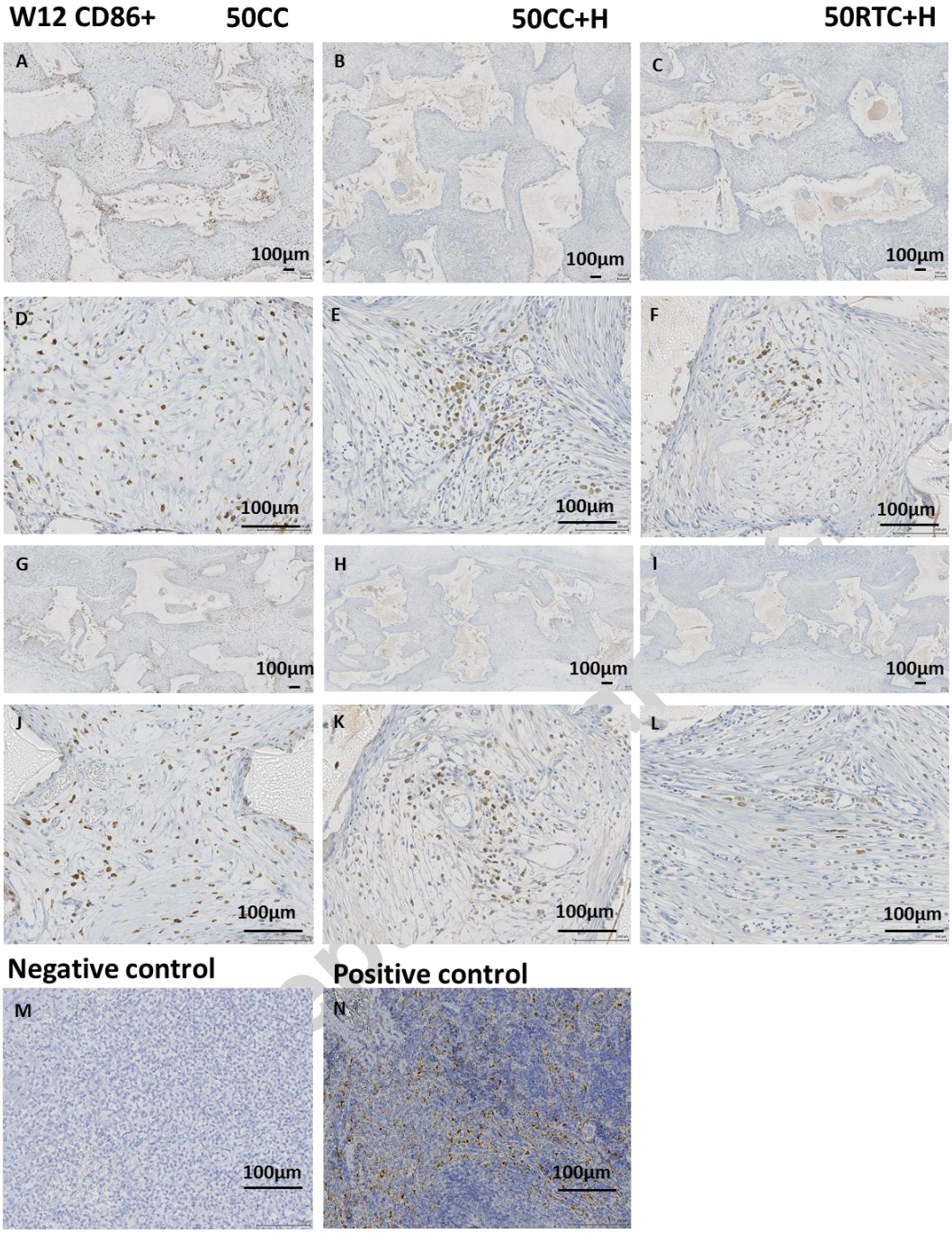


**Figure 7 Immunohistochemistry of the host macrophage response towards scaffolds *in vivo* at week 12**. Tissue integration of middle-in-plane (A-F) and cross-sectional view (G-L) of the scaffolds by CD86 (M1 macrophage marker) staining at (A-C, G-I) ×4 and (D-F, J-L) ×20 magnifications. (M) Negative control (rat appendix); (N) positive control (rat liver). Scale bar: 100 µm.

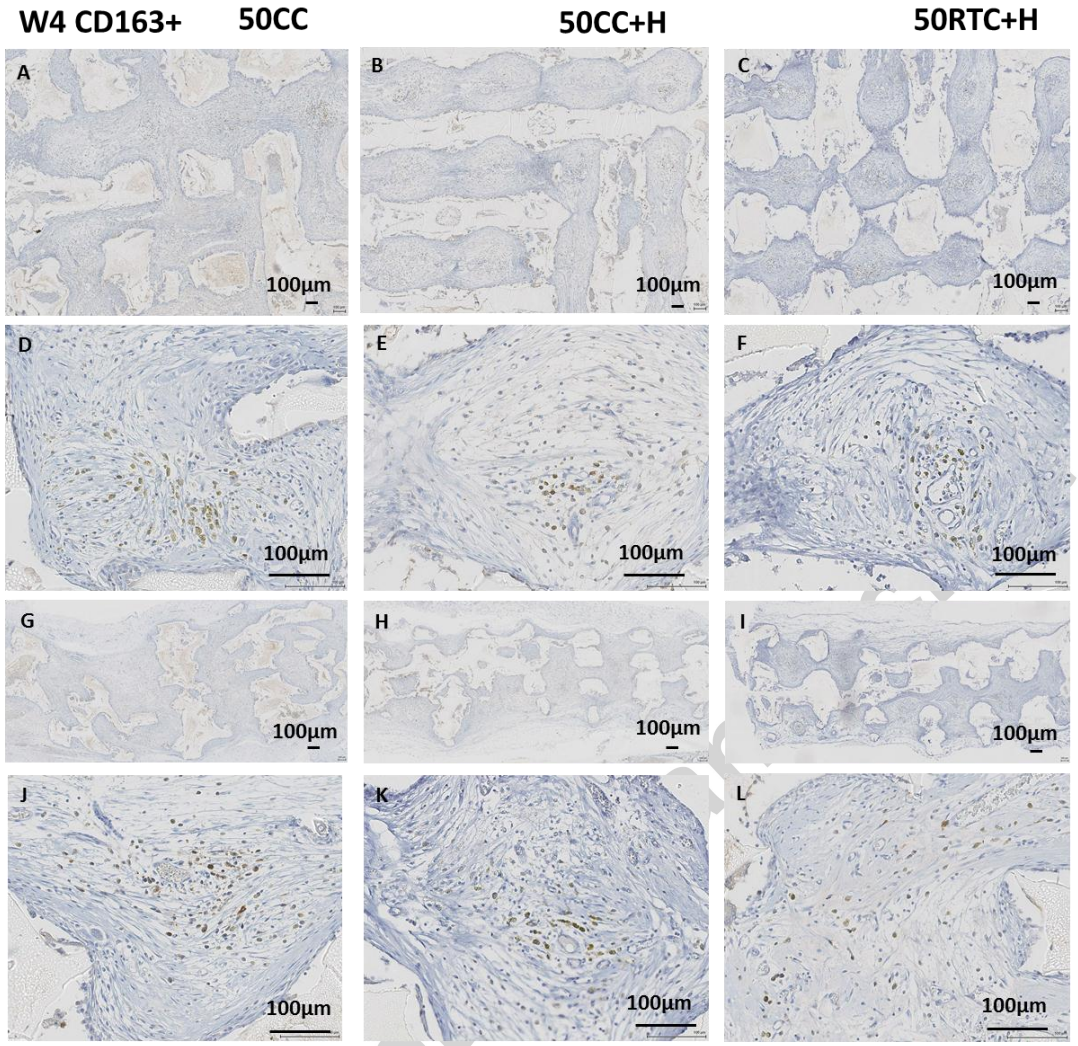


**Figure 8 Immunohistochemistry of the host macrophage response towards scaffolds *in vivo* at week 4**. Tissue integration of middle-in-plane (A-F) and cross-sectional view (G-L) of the scaffolds by CD163 (M2 macrophage marker) staining at (A-C, G-I) ×4 and (D-F, J-L) ×20 magnifications.

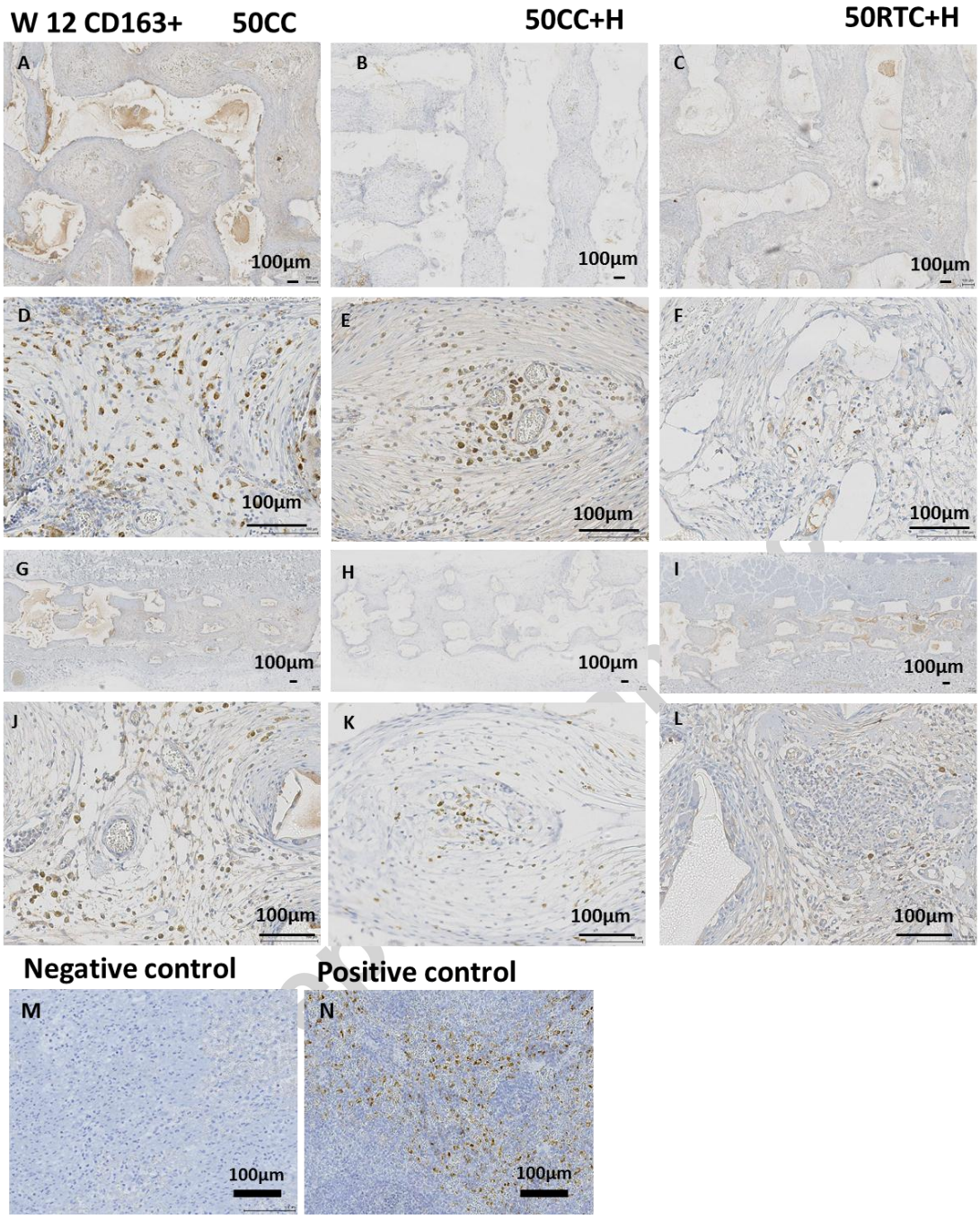


**Figure 9 Immunohistochemistry of the host macrophage response towards scaffolds *in vivo* at weeks 12**. Tissue integration of middle-in-plane (A-F) and cross-sectional view (G-L) of the scaffolds by CD163 (M2 macrophage marker) staining at (A-C, G-I) ×4 and (D-F, J-L) ×20 magnifications. (M) Negative control (rat appendix); (N) positive control (rat liver). Scale bar: 100 µm.

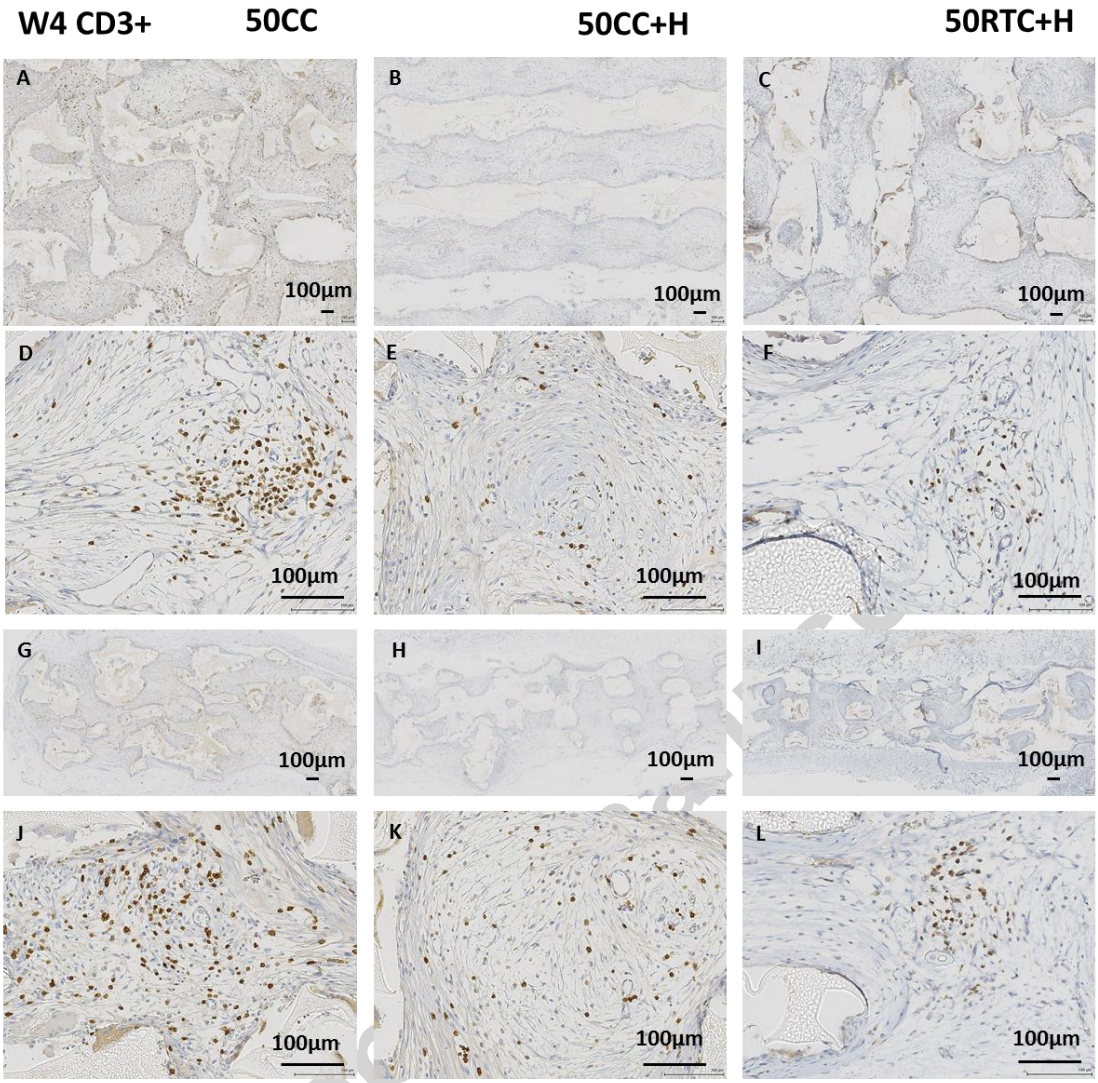


**Figure 10 Immunohistochemistry of the host T lymphocyte response towards scaffolds *in vivo* at week 4**. Tissue integration of middle-in-plane (A-F) and cross-sectional view (G-L) of the scaffolds by CD3 (T lymphocyte marker) staining at (A-C, G-L) ×4 and (D-F, J-L) ×40 magnifications.

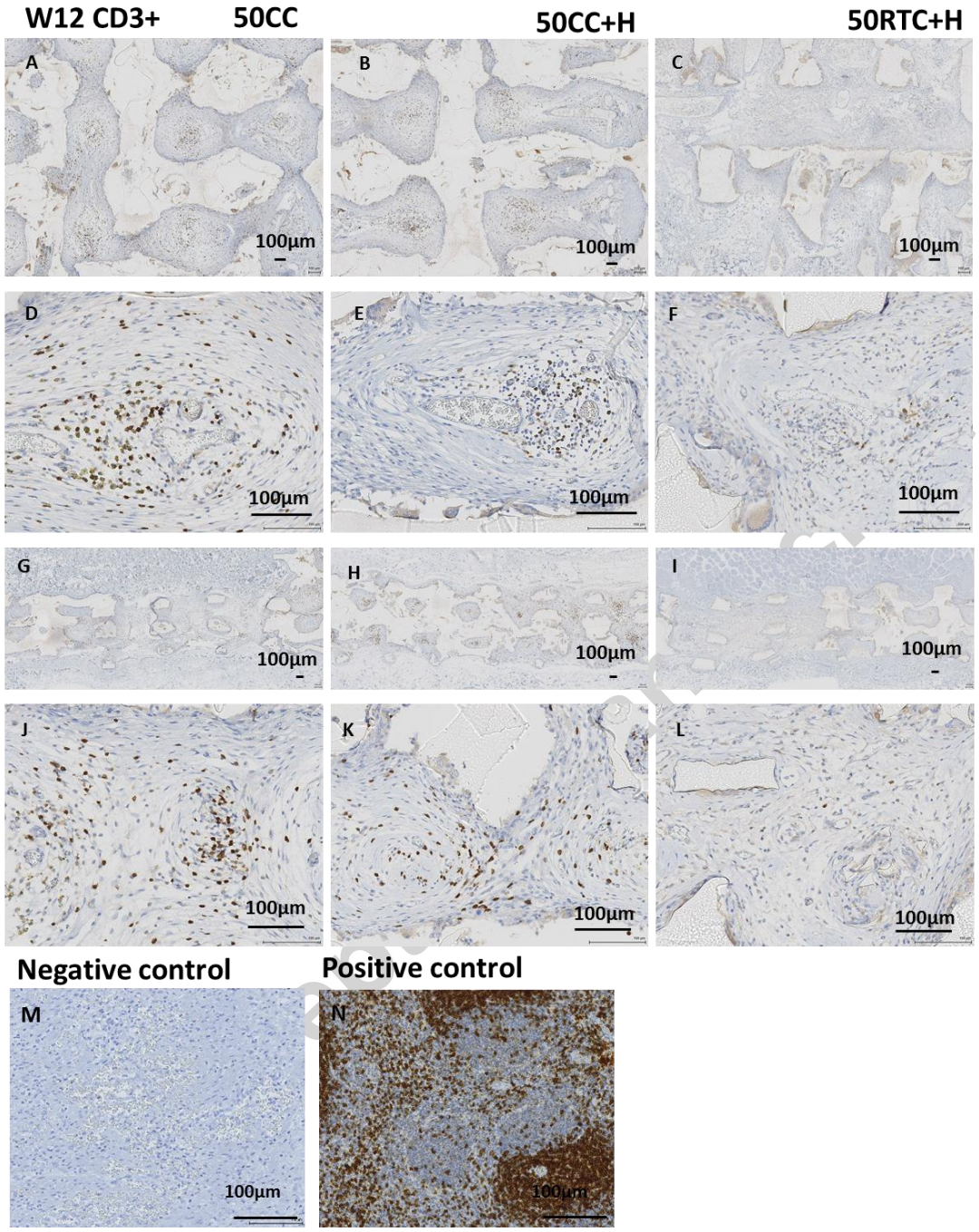


**Figure 11 Immunohistochemistry of the host T lymphocyte response towards scaffolds *in vivo* at week 12**. Tissue integration of middle-in-plane (A-F) and cross-sectional view (G-L) of the scaffolds by CD3 (T lymphocyte marker) staining at (A-C, G-I) ×4 and (D-F, J-L) ×20 magnifications. (M) Negative control (rat appendix); (N) positive control (rat spleen). Scale bar: 100 µm.

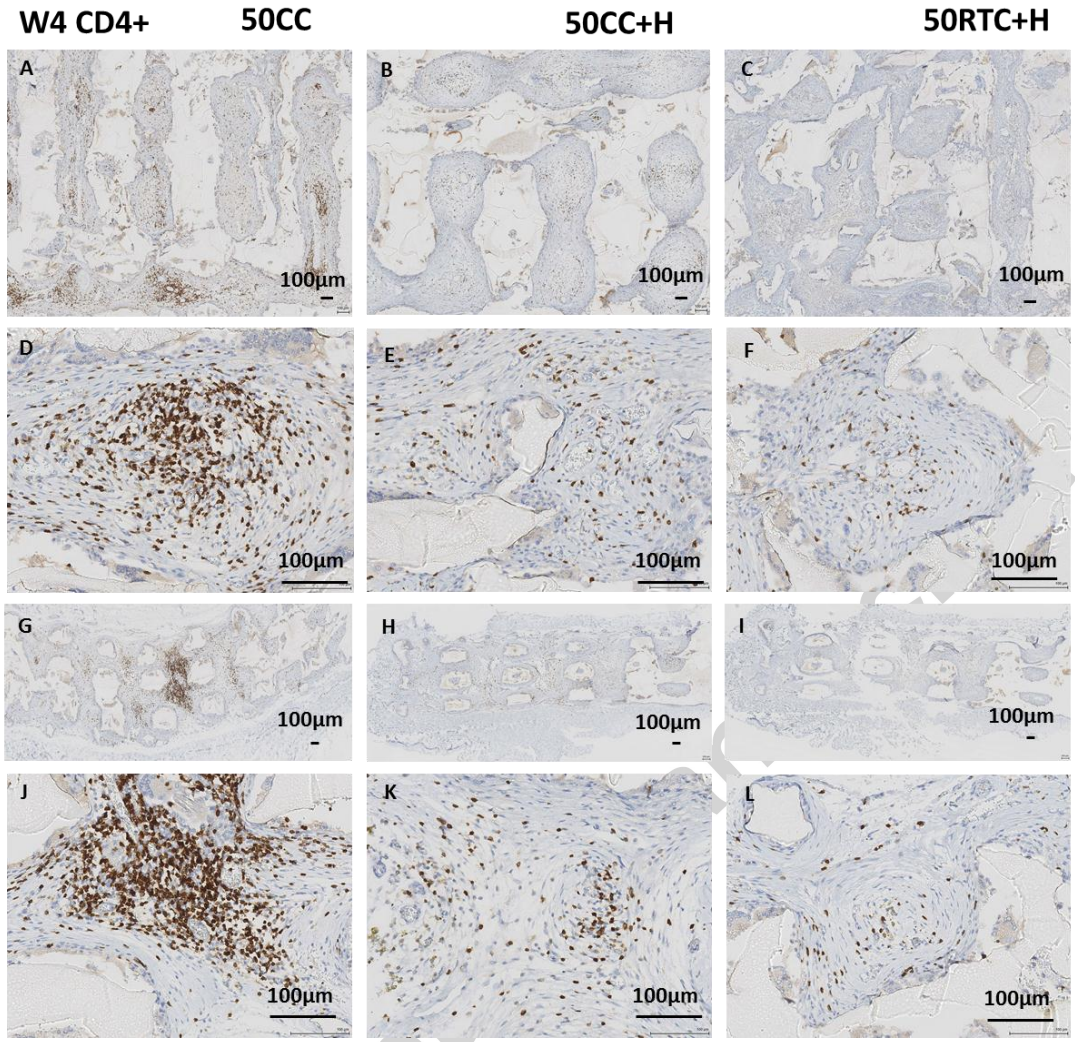


**Figure 12 Immunohistochemistry of the host T lymphocyte response towards scaffolds *in vivo* at week 4.** Tissue integration of middle-in-plane (A-F) and cross-sectional view (G-L) of the scaffolds by CD4 (T lymphocyte marker) staining at (A-C, G-I) ×4 and (D-F, J-L) ×20 magnifications.

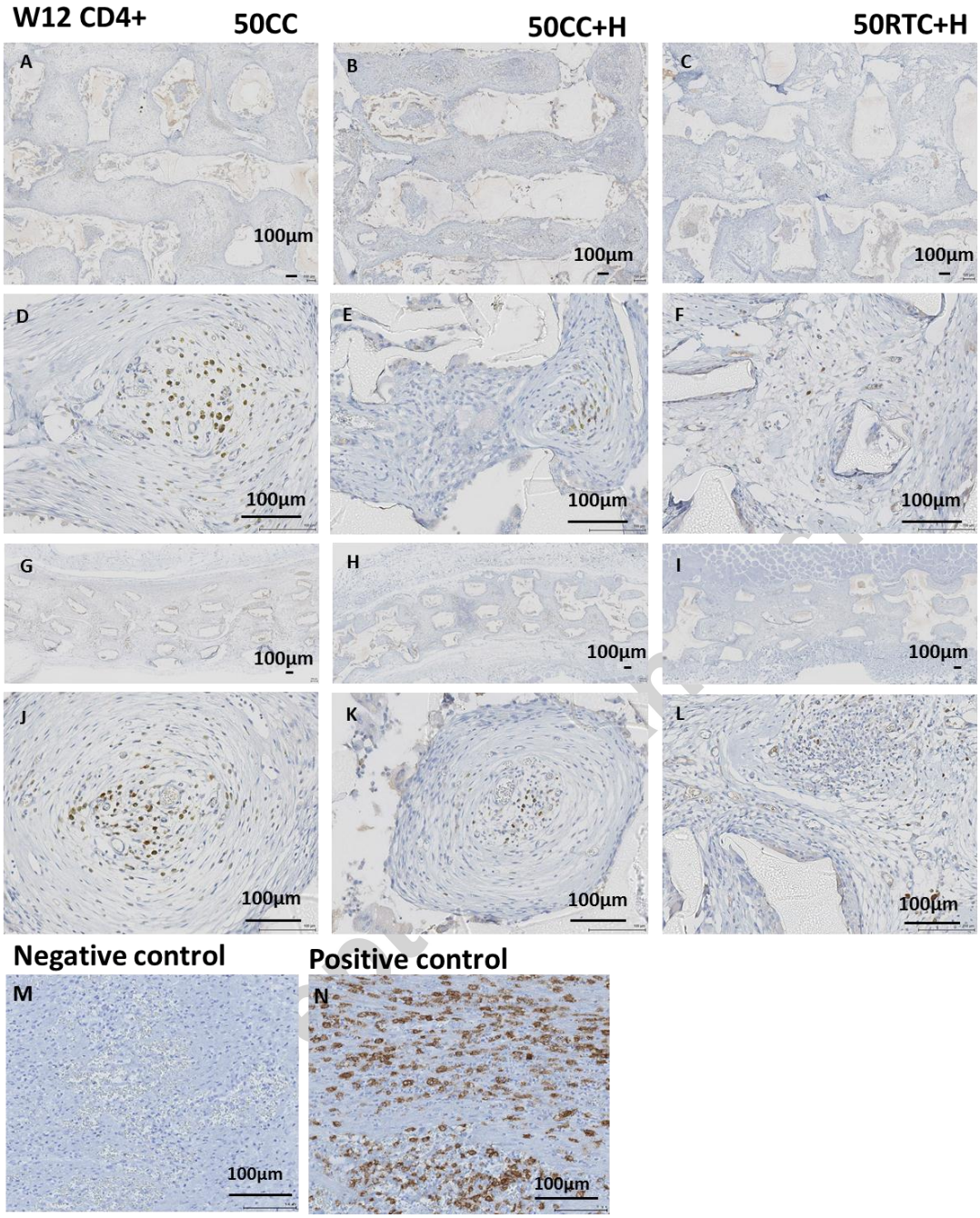


**Figure 13 Immunohistochemistry of the host T lymphocyte response towards scaffolds *in vivo* at week 12.** Tissue integration of middle-in-plane (A-F) and cross-sectional view (G-L) of the scaffolds by CD4 (T lymphocyte marker) staining at (A-C, G-I) ×4 and (D-F, J-L) ×20 magnifications. (M) Negative control (rat appendix); (N) positive control (rat spleen). Scale bar: 100 µm.

## 2. Experimental Design, Materials and Methods

### 2.1 Fabrication of thermoresponsive PUU-POSS scaffolds

A 3D-TIPS technique, based on reverse 3D printing and phase separation of polymer solution, as described in [1], was used to manufacture PUU-POSS scaffolds (50% infill density) at different thermal conditions (50CC, 50CC+H and 50RTC+H).

### 2.2 Characterization of the scaffolds prior to implantation

An Instron 5655 was applied to test static tensile mechanical properties of the scaffolds, before and after incubation over 28 days at body temperature, as described in [1], as well the explants after implantation in rats for 4, 8 and 12 weeks. The dimensions of the printed preforms and the scaffold as produced were also measured and estimated.

### 2.2 Characterization of the scaffold explants

As detailed in [1], the scaffolds were subcutaneously implanted in adult male rats and harvested at different time points. The physico-mechanical properties (i.e. tensile properties and phase structure) were then analyzed with an Instron 5655 tester and an X-ray diffractometer. Sectioning and histological staining (i.e. H&E and M&T) were carried out, and collagen fiber formation and tissue ingrowth orientation was quantified as previously described [1]. Immunofluorescent staining against capillary marker CD31, macrophage markers CD86/CD68/CD163 and T-cell makers CD3/CD4 was carried out, and the number of positive stained cells was quantified as described in [1].

**Acknowledgements**
The authors acknowledge financial support by the Engineering and Physical Sciences Research Council in the United Kingdom (EPSRC), grant Nos. EP/L020904/1, EP/M026884/1 and EP/R02961X/1.

**Competing interests**
The authors declare no potential conflict of interests with respect to the research, authorship and/or publication of this article.

**References**
[1] L. Wu, A. Magaz, E. Maughan, N. Oliver, A. Darbyshire, M. Loizidou, M. Emberton, M. Birchall, W. Song, Cellular responses to thermoresponsive stiffness memory elastomer nanohybrid scaffolds by 3D-TIPS, Acta Biomater. (2018). doi:10.1016/j.actbio.2018.12.019.